Inorg. Chem. **2002**, *41*, 1454–1463

Quantitative Reactivity Model for the Hydration of Carbon Dioxide by Biomimetic Zinc Complexes[⊥]

Michael Bräuer,[†] J. Luis Pérez-Lustres,[‡] Jennie Weston,[§] and Ernst Anders*[,§]

Continental AG, Jedekamp 30, 30419 Hannover, Germany, Departamento de Química Física, Facultade de Química, Universidade de Santiago de Compostela, E-15706 Santiago de Compostela, Spain, and Institut für Organische Chemie und Makromolekulare Chemie der Friedrich-Schiller-Universität, Humboldtstrasse 10, D-07743 Jena, Germany

Received September 15, 2000

A quantitative structure–reactivity relationship has been derived from the results of B3LYP/6-311+G* calculations on the hydration of carbon dioxide by a series of zinc complexes designed to mimic carbonic anhydrase. The reaction mechanism found is general for all complexes investigated. The reaction exhibits a low (4–6 kcal/mol) activation energy and is exothermic by about 8 kcal/mol. The calculations suggest an equilibrium between Lipscomb and Lindskog intermediates. The effectiveness of the catalysis is a function of the nucleophilicity of the zinc-bound hydroxide and the nucleofugicity of the zinc-bound bicarbonate. Hydrogen bridging of the bicarbonate to NH moieties in the ligands also plays an important role.

Introduction

Carbonic anhydrase is a ubiquitous zinc enzyme which catalyzes the reversible hydration of CO_2.[1] The equilibrium position of this reaction is pH dependent. Whereas, hydration of CO_2 takes place at pH > 7, the dehydration of bicarbonate predominates at pH < 7. Out of the seven isoenzymes found so far,[1e] human carbonic anhydrase II (HCA II) is the most efficient one with turnover numbers of 10^6 s^{-1} at pH = 9 and 25 °C.[1g] The polypeptide chain of HCA II is composed of more than 260 amino acids and forms an ellipsoid[2] with the dimensions 55 × 42 × 39 Å^3 and has a molecular weight of 30 000. The active site lies at the bottom of a conical cavity which is 16 Å deep and 15 Å wide at the opening. The zinc cation is surrounded by three imidazole ligands (His94, His96, and His119). An additional water molecule lies at the bottom of the cavity. The arrangement of the amino acids results in a hydrophilic and a hydrophobic region in the cavity. The hydrophilic region contains His64 and seven additional water molecules and is responsible for the migration of the proton from the zinc-bound water to the external medium. The hydrophobic site is thought to provide binding pockets for fast CO_2 transport to and from the blood stream.[2c]

In the absence of carbonic anhydrase, the reaction of CO_2 proceeds with an activation energy of 17.7 kcal/mol in neutral water[3] (eq 1) and 13.1 kcal/mol in basic aqueous solution[4] (eq 2).

$$CO_2 + H_2O \rightarrow H_2CO_3 \quad (1)$$

$$CO_2 + OH^- \rightleftharpoons HCO_3^- \quad (2)$$

HCA II catalyzes the reaction with rates up to 10^7 times higher than in the uncatalyzed case. A plausible reaction mechanism[5] for the mode of action has been proposed: (i) The zinc-bound hydroxide {[LZn−OH]$^+$} first attacks the carbon dioxide to yield bicarbonate. (ii) The zinc-bound

[⊥] Dedicated to Professor Lutz F. Tietze on the occasion of his 60th birthday.

[†] Continental AG (Trainee Pool, Spring 2000).

[‡] Universidade de Santiago de Compostela.

[§] Institut für Organische Chemie und Makromolekulare Chemie der Friedrich-Schiller-Universität. E-mail: c5eran@uni-jena.de (E.A.); c9weje@uni-jena.de (J.W.). Fax: (+49)3641-948212.

(1) (a) Davis, R. P. *J. Am. Chem. Soc.* **1958**, *80*, 5209. (b) Davis, R. P. *J. Am. Chem. Soc.* **1959**, *81*, 5674. (c) Coleman, J. E. *J. Biol. Chem.* **1967**, *242*, 5212. (d) Steiner, H.; Jonsson, B. H.; Lindskog, S. *FEBS Lett.* **1976**, *16*, 62. (e) Silverman, D. N.; Lindskog, S.; Tu, C. K.; Wynns, G. C. *J. Am. Chem. Soc.* **1979**, *101*, 6734. (f) Rowlett, R. S.; Silverman, D. N. *J. Am. Chem. Soc.* **1982**, *104*, 6737. (g) Lindskog, S. *Carbonic Anhydrase*; Lindskog, S., Ed.; Wiley: New York, 1983; p 77. (h) Liang, J. Y.; Lipscomb, W. N. *Biochemistry* **1987**, *26*, 5293. (i) Silverman, D. N.; Linsdkog, S. *Acc. Chem. Res.* **1988**, *21*, 30. (k) Liang, J. Y.; Lipscomb, W. N. *Biochemistry* **1988**, *27*, 8676. (l) Christianson, D. W. *Adv. Protein Chem.* **1991**, *42*, 281.

(2) (a) Eriksson, A. E.; Jones, T. A.; Liljas, A. *Proteins* **1988**, *4*, 274. (b) Håkansson, M.; Carlsson, L.; Svensson, A.; Liljas, A. *J. Mol. Biol.* **1992**, *227*, 1192. (c) Vallee, B. L.; Auld, D. S. *Acc. Chem. Res.* **1993**, *26*, 543.

(3) Magid, E.; Turbeck, B. O. *Biochim. Biophys. Acta* **1968**, *165*, 515.

(4) Pinsent, B. R. W.; Pearson, L.; Roughton, F. J. W. *Trans. Faraday Soc.* **1956**, *52*, 1512.

10.1021/ic0010510 CCC: $22.00
Published on Web 02/20/2002

Scheme 1. Lipscomb and Lindskog mechanisms for the Rearrangement of the Zinc-Bound Bicarbonate

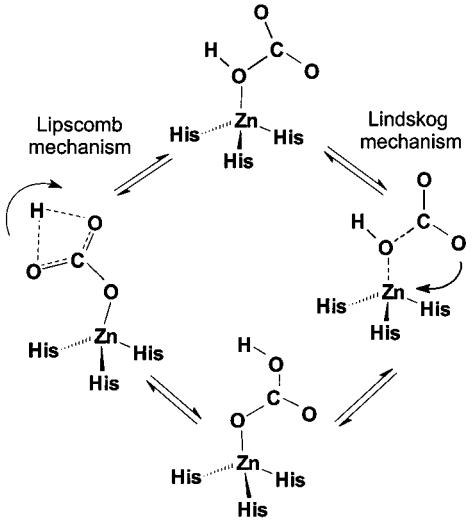

bicarbonate is then displaced by a water molecule, and in the last step, (iii) this water molecule ($pK_a \sim 7$) is finally deprotonated to regenerate the $[LZn-OH]^+$ catalyst.

Apart from numerous experimental studies,[6] computer simulations have contributed significantly to our present knowledge of the reaction mechanism. The entire spectrum of molecular modeling ranging from molecular dynamics[7] over the application of semiempirical methods[8] and including ab initio and DFT calculations[9,10] has been applied in these investigations. Because of the general acceptance of the hydroxide mechanism, the most recent publications have focused more on the mechanism of intramolecular proton shifts in individual steps of the catalytic reaction.[6,7] Special attention has been paid to the mechanistic details of the rearrangement of the bicarbonate in step (i) of the reaction (Scheme 1). The debate whether an intramolecular proton transfer (Lipscomp mechanism [8,9,11]) or an internal rotation

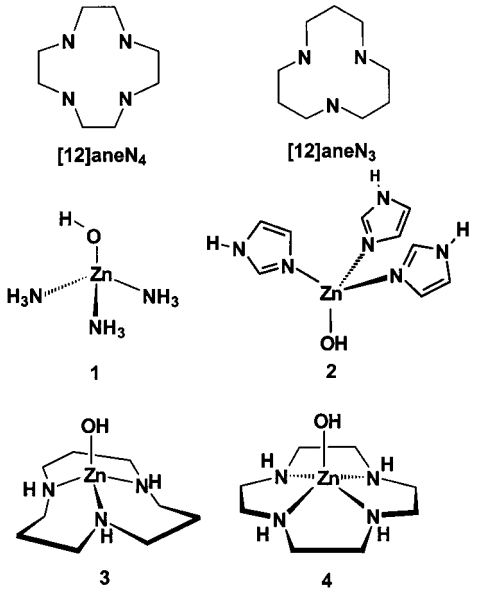

Figure 1. Ligands and complexes which were used for the modeling of carbonic anhydrase.

of the bicarbonate (Lindskog mechanism[1i,6]) takes place or not could not be completely settled until now. [8,9]

An important contribution to the detailed understanding of the catalytic activity of the enzyme was made via experimental investigations on suitable model systems.[12] Complexes with a structural resemblance to the native enzyme were synthesized and characterized as regarding their activity toward HCA II. Among these studies, the work of Vahrenkamp[13] and Kimura[14] are especially worth mentioning. Kimura's macrocyclic donor ligands such as 1,4,7,10-tetraazacylododecane ([12]aneN$_4$) and 1,5,9-triazacyclododecane ([12]aneN$_3$; see Figure 1) were used to model the protein environment of carbonic anhydrase. Kinetic measurements in aqueous solution on the activity of these complexes were carried out by van Eldik[15] et al. They observed a remarkable difference in the performance. Both enzyme models are prin-

(5) Lindskog, S.; Coleman, J. E. *Proc. Natl. Acad. Sci. U.S.A.* **1973**, *70*, 2505.
(6) (a) Bertini, I.; Luchinat, C. *Acc. Chem. Res.* **1983**, *16*, 272. (b) Zhang, X.; Hubbard, C. D.; v. Eldik, R. *J. Phys. Chem.* **1996**, *100*, 9161. (c) Eriksson, A. E.; Jones, T. A.; Liljas, A. *Proteins* **1988**, *4*, 274. (d) Håkansson, M.; Carlsson, L.; Svensson, L. A.; Liljas, A. *J. Mol. Biol.* **1992**, *227*, 1192.
(7) (a) Merz, K. M., Jr. *J. Mol. Biol*. **1990**, *214*, 799. (b) Merz, K. M., Jr. *J. Am. Chem. Soc.* **1991**, *113*, 406. (c) Merz, K. M., Jr.; Banci, L. *J. Phys. Chem.* **1996**, *100*, 17414. (d) Merz, K. M., Jr.; Banci, L. *J. Am. Chem. Soc.* **1997**, *119*, 863. (e) Toba, S.; Colombo, G.; Merz, K. M., Jr. *J. Am. Chem. Soc.* **1999**, *121*, 2290. (f) Zheng, Y.-J.; Merz, K. M., Jr. *J. Am. Chem. Soc.* **1992**, *114*, 10498−10507. (g) Garmer, D. R. *J. Phys. Chem. B* **1997**, *101*, 2945−2953.
(8) (a) Liang, J.-Y.; Lipscomb, W. N. *Int. J. Quantum Chem.* **1989**, *XXXVI*, 299. (b) Hartmann, M.; Merz, K. M., Jr.; Clark, T.; van Eldik, R. *J. Mol. Model.* **1998**, *4*, 355. (c) Merz, K. M., Jr.; Hoffmann, R.; Dewar, M. J. S. *J. Am. Chem. Soc.* **1989**, *111*, 5636−5649.
(9) (a) Pullman, A.; Demoulin, D. *Int. J. Quantum Chem.* **1979**, *XVI*, 641. (b) Cini, R.; Musaev, D. G.; Marzilli, L. G.; Morokuma, K. *THEOCHEM* **1997**, *392*, 55. (c) Muguruma, C. *THEOCHEM* **1999**, *461*, 439. (d) Jacob, O.; Cardenas, R.; Tapia, O. *J. Am. Chem. Soc.* **1990**, *112*, 8692−8705. (e) Krauss, M.; Garmer, D. R. *J. Am. Chem. Soc.* **1991**, *113*, 6426−6435. (f) Solá, M.; Lledós, A.; Duran, M.; Bertrán, J. *J. Am. Chem. Soc.* **1992**, *114*, 869−877. (g) Zheng, Y.-J.; Merz, K. M., Jr. *J. Am. Chem. Soc.* **1992**, *114*, 10498−10507. (h) Lu, D.; Voth, G. A. *J. Am. Chem. Soc.* **1998**, *120*, 4006−4014.
(10) Mauksch, M., Bräuer, M., Weston, J., Anders, E. *ChemBioChem* **2001**, *No. 3*, 190−198.
(11) Liang, J. Y.; Lipscomb, W. N. *Biochemistry* **1988**, *27*, 8676.
(12) (a) Woolley, P. *Nature* **1975**, *258*, 677. (b) Looney, A.; Han, R.; McNeill, K.; Parkin, G. *J. Am. Chem. Soc.* **1993**, *115*, 4690. (c) Kitajima, N.; Hikichi, S.; Tanaka, M.; Moro-oka, Y. *J. Am. Chem. Soc.* **1993**, *115*, 5496. (d) Bazzicalupi, C.; Bencini, A.; Bencini, A.; Bianchi, A.; Corana, F.; Fusi, V.; Giorgi, C.; Paoli, P.; Paoletti, P.; Valtancoli, B.; Zanchini, C. *Inorg. Chem.* **1996**, *35*, 5540. (e) Nakata, K.; Uddin, M. K.; Ogawa, K.; Ichikawa, K. *Chem. Lett.* **1997**, 991. (f) Xu, X.; Lajmi, A. R.; Canary, J. W. *Chem. Commun.* **1998**, 2701.
(13) (a) Alfasser, R.; Ruf, M.; Trofimenko, S.; Vahrenkamp, H. *Chem. Ber.* **1993**, *126*, 703. (b) Gregorzik, R.; Hartmann, U.; Vahrenkamp, H. *Chem. Ber.* **1994**, *127*, 2117. (c) Hartmann, U.; Gregorzik, R.; Vahrenkamp, H. *Chem. Ber*. **1994**, *127*, 2123. (d) Gockel, P.; Vogler, R.; Vahrenkamp, H. *Chem. Ber.* **1996**, *129*, 887. (e) Ruf, M.; Schell, F. A.; Walz, R.; Vahrenkamp, H. *Chem. Ber./Recl.* **1997**, *130*, 101. (f) Gockel, P.; Vahrenkamp, H. *Chem. Ber.* **1996**, *129*, 1243. (g) Ruf, M.; Vahrenkamp, H. *Chem. Ber.* **1996**, *129*, 1025. (h) Ruf, M.; Burth, R.; Weis, K.; Vahrenkamp, H. *Chem. Ber.* **1996**, *129*, 1251. (i) Titze, C.; Hermann, J.; Vahrenkamp, H. *Chem. Ber.***1995**, *128*, 1095−1103.
(14) (a) Kimura, E.; Shiota, T.; Koike, T.; Shiro, M.; Mutsuo, M. *J. Am. Chem. Soc.* **1990**, *112*, 5805. (b) Sakurai, M.; Furuki, T.; Inoue, Y. *J. Phys. Chem.* **1995**, *99*, 17789. (c) Kimura, E.; Koike, T. *Adv. Inorg. Chem.* **1997**, *44*, 229. (d) Suh, J.; Son, S. J.; Suh, M. P. *Inorg. Chem.* **1998**, *37*, 4872−4877. (e) Kimura, E.; Koike, T.; Toriumi, K. *Inorg. Chem.* **1988**, *27*, 3687−3688. (f) Kimura, E.; Kurosaki, H.; Koike, T.; Toriumi, K. *J. Inclusion Phenom. Macrocyclic Chem.* **1992**, *12*, 377−387. (g) Kimura, E.; Nakamura, I.; Koike, T.; Shionoya, M. *Struct. Bonding (Berlin)* **1997**, *89*, 1−28.

Table 1. Selected Properties of the Carbonic Anhydrase Model Complexes as Compared to the Native Enzyme[15]

	$K_{FORWARD}$ [s^{-1} M^{-1}]	K_{BACK} [s^{-1} M^{-1}]	pK_a
HCA II	1.06×10^6	2.2×10^5	6.8
$[Zn[12]aneN_4OH]^+$	3.3×10^3	51	8.1
$[Zn[12]aneN_3OH]^+$	581	4.8	7.5

cipally able to reversibly catalyze the CO_2 hydration. Despite the closer structural resemblance of $[Zn[12]aneN_3OH]^+$ (**3**) to the native enzyme because of its tetrahedral-like coordination, $[Zn[12]aneN_4OH]^+$ (**4**) displays a higher catalytic activity which can reach up to 30% of some native isoenzymes.[15] Apart from the catalytic activity, summarized for these enzyme models in Table 1, the corresponding water complexes $[LZnOH_2]^{2+}$ can be deprotonated at physiologically relevant pH values.

In this study, we calculated the reaction of the model complexes in Figure 1 with CO_2 using ab initio and DFT methods. On one hand, we wanted to present a mechanistic study on an appropriate level of theory with a variety of model compounds for comparison. On the other hand, we wanted to derive parameters which characterize the activity of such systems. The results presented here should contribute to the future understanding of the reaction mechanism as well as clarify general aspects of enzyme controlled reactions and stimulate investigations on new model systems.

The $[Zn(NH_3)_3OH]^+$ complex (**1**) is the most thoroughly investigated CA model system and, because of its moderate size, can be treated with sophisticated quantum chemical methods.[7c,e,10] We recently published a complete catalytic cycle for this model complex calculated at the B3LYP/6-311+G* level.[10] We then compared these results[10] to B3LYP/6-311+G*//RHF/6-311+G* single point calculations in order to assess the reliability of this approximation (which had to be applied for all larger systems, cf., Computational Details). We then investigated the **2**/CO_2 system (Scheme 2), because the tris-imidazole complex **2** shows the closest structural simularity to the active site of the native enzyme. Both zinc complexes **1** and **2** form tetrahedral structures containing three nitrogen donor ligands and one hydroxide ion without significant sterical restrictions. Because of their similar coordination geometries, we could directly compare the influence of sp^2- and sp^3-hybridized nitrogen donor ligands on the catalytic activity. Finally, the existence of reliable experimental data on the activity of $[Zn([12]aneN_3)OH]^+$ (complex **3**) and $[Zn([12]aneN_4)OH]^+$ (complex **4**) enabled us to compare the properties of these two complexes and to draw conclusions regarding the parameters controlling their respective activities.

Computational Details

Full conformational searches using the program SPARTAN[16] were performed for all species of interest using the semiempirical methods MNDO/d,[17] AM1,[18] and PM3.[19] All three methods were employed since a recent investigation[20] has shown that none of the three methods can be relied upon to correctly predict the overall structure of organozinc compounds, especially when multiple zinc−heteroatom bonds are present. PM3, for example, fails to describe Zn−O interactions but correctly describes many bio-organic complexes.[20] AM1 behaves similarly to PM3; the average errors found, however, are ∼30% larger than for PM3.[20] The semiempirical structures served as starting geometries for optimizations at the HF/6-311+G* level of theory. All HF and DFT calculations were performed using the GAUSSIAN 98[21] suite of programs. The nature of all stationary points was then characterized by harmonic frequency analysis.[22] B3LYP/6-311+G* single point calculations were then performed on the HF geometries in order to partially

Scheme 2. CO_2 Fixation and Transformation as Illustrated for Catalyst **2**; Relative Energies Are Given in kcal/mol and Were Calculated at the B3LYP/6-311+G*//RHF/6-311+G* Level

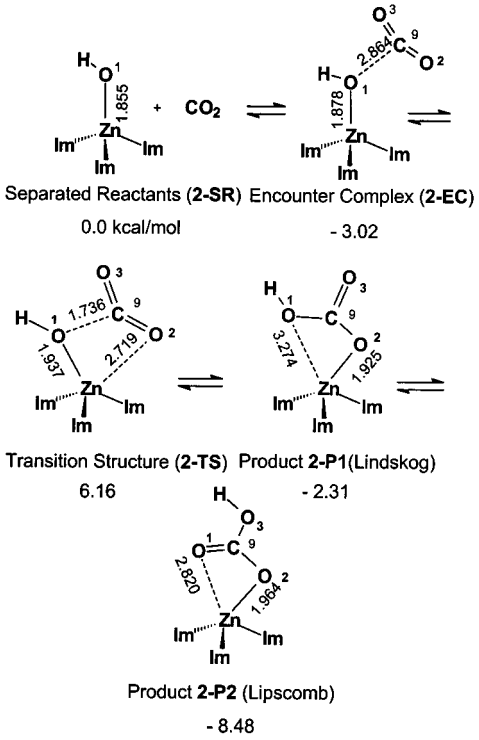

(15) (a) Zhang, X.; v. Eldik, R.; Koike, T.; Kimura, E. *Inorg. Chem.* **1993**, *32*, 5749. (b) Zhang, X.; v. Eldik, R. *Inorg. Chem.* **1995**, *34*, 5606.
(16) Spartan is available from Wavefunction, Inc., 19491 von Karman Ave., Suite 370, Irvine CA.
(17) Thiel, W.; Voityuk, A. A. *J. Phys. Chem.* **1996**, *100*, 616. Thiel, W.; Voityuk, A. A. *Theor. Chim. Acta* **1992**, *81*, 391. Dewar, M. J. S.; Merz, K. M., Jr. *Organometallics* **1986**, *5*, 1494. Dewar, M. J. S.; Thiel, W. *J. Am. Chem. Soc.* **1977**, *99*, 4899.
(18) Dewar, M. J. S.; Merz, K. M., Jr. *Organometallics* **1988**, *7*, 522. Dewar, M. J. S.; Zoebisch, E. G.; Healy, E. F.; Stewart, J. J. P. *J. Am. Chem. Soc.* **1985**, *107*, 3902.
(19) Stewart, J. J. P. *J. Comput. Chem.* **1989**, *10*, 209; 221.
(20) Bräuer, M.; Kunert, M.; Dinjus, E.; Klussmann, M.; Döring, M.; Görls, H.; Anders, E. *THEOCHEM* **2000**, *505*, 289.
(21) Frisch, M. J.; Trucks, G. W.; Schlegel, H. B.; Scuseria, G. E.; Robb, M. A.; Cheeseman, J. R.; Zakrzewski, V. G.; Montgomery, J. A., Jr.; Stratmann, R. E.; Burant, J. C.; Dapprich, S.; Millam, J. M.; Daniels, A. D.; Kudin, K. N.; Strain, M. C.; Farkas, O.; Tomasi, J.; Barone, V.; Cossi, M.; Cammi, R.; Mennucci, B.; Pomelli, C.; Adamo, C.; Clifford, S.; Ochterski, J.; Petersson, G. A.; Ayala, P. Y.; Cui, Q.; Morokuma, K.; Malick, D. K.; Rabuck, A. D.; Raghavachari, K.; Foresman, J. B.; Cioslowski, J.; Ortiz, J. V.; Stefanov, B. B.; Liu, G.; Liashenko, A.; Piskorz, P.; Komaromi, I.; Gomperts, R.; Martin, R. L.; Fox, D. J.; Keith, T.; Al-Laham, M. A.; Peng, C. Y.; Nanayakkara, A.; Gonzalez, C.; Challacombe, M.; Gill, P. M. W.; Johnson, B. G.; Chen, W.; Wong, M. W.; Andres, J. L.; Head-Gordon, M.; Replogle, E. S.; Pople, J. A. *Gaussian 98*, revision A.5; Gaussian, Inc.: Pittsburgh, PA, 1998.
(22) Pulay, P. In *Ab Initio Methods in Quantum Chemistry*; Lawley, K. P., Ed.; Wiley: New York, 1987; p 241.

account for electron correlation. Full geometry optimizations together with harmonic frequency analysis were then performed at the B3LYP/6-311+G* level for all stationary points of complex **1**. These calculations give results that are almost identical to the single point calculations (Table 4), thus justifying this procedure for the larger systems. The excellent performance of the B3LYP functional was demonstrated by comparing the results for the model system $[Zn-OH]^+$ with those obtained at the CCSD(T)//6-311+G* level of theory (see Table 4 for details). Semiempirical calculations were carried out using the MOPAC6[23] program package. The PM3-COSMO[24] solvation model, as implemented in VAMP,[25] was used to estimate the structural and energetic changes in aqueous solution as compared to the gas phase. The relative stabilities and energies of formation reported in this article contain a correction for the zero point vibrational energy (a scaling factor of 0.91 was employed for the HF results;[26] the B3LYP results were not scaled). Reed and Weinhold's natural bond orbital (NBO) analysis[27] was used to calculate changes in the atomic charges along the course of the reaction path.

Results and Discussion

Reaction Mechanism. The intermediate structural motifs, as depicted explicitly for the **2**/CO_2 system in Scheme 2, were calculated for all selected complexes in order to model the enzyme function. Table 2 contains structural parameters for the stationary points (**EC**, **TS**, **P1**, and **P2**) of the four model systems. Selected results of the NBO analyses are summarized in Table 3. Many authors have reported calculations on the carbonic anhydrase mechanism under inclusion of additional water molecules.[7a−e,7g,9f] These solvent molecules may cause an easier detachment of the bicarbonate in the last step of the catalytic cycle. In the present work, we concentrated on the electronic effects of different ligand spheres on the reactivity of model complexes. Our calculations refer to gas-phase conditions; solvent effects in aqueous solution were simulated using the B3LYP-COSMO and the PM3-COSMO method. The relevance of five-coordinated intermediates under specific inclusion of external water molecules is the topic of a parallel investigation.[28]

In the first step of the catalysis, the separated reactants form an encounter complex (**EC**, cf. Scheme 2; for information regarding catalysts **1**, **3**, and **4**, cf. Table 2), in which a lone pair on the zinc-bound hydroxide interacts with the carbon atom of CO_2. Although the existence of such electrostatic encounter complexes in solution must be questioned (vide infra), they constitute minima on the potential energy surface of the undisturbed system in the gas phase and thus provide important information on the extent of fundamental interactions. In the next step of the reaction, the primary bicarbonate complex **P1** (Lindskog) is formed via the transition structure **TS**. For all model compounds studied here, the transition structure **TS** represents the maximum in the potential energy of the catalytic cycle and is thus expected to be the rate-limiting step in the formation of hydrogen carbonate. Complex **P1** then rearranges to form the more stable complex **P2**. In the meantime, there is experimental evidence for the intermediate formation of a $Co(OH)(CO_2H)$ complex in a cobalt substituted HCA

Table 2. Selected Bond Lengths Calculated at the RHF/6-311+G* Level for the Carbonic Anhydrase Model Complexes **1**−**4** and the Corresponding Stationary Points **EC**, **TS**, **P1**, and **P2** of the Catalytic Cycle[a]

	1	**2**	**3**	**3′**	**4**
		free catalyst			
Zn−O1	1.833	1.855	1.829		1.837
		EC			
Zn−O2	3.761	4.453	3.716		3.657
Zn−O1	1.841	1.878	1.842		1.852
O1−C9	2.740	2.863	2.723		2.700
		TS			
Zn−O1	1.932	1.937	1.934		1.936
Zn−O2	2.368	2.717	2.384		2.579
O1−C9	1.743	1.736	1.754		1.716
H···O=C=O	2.497	2.252	2.813		2.497
		P1			
Zn−O1	2.832	3.274	2.992	2.751	2.929
Zn−O2	1.901	1.925	1.885	1.897	1.897
O1−C9	1.378	1.359	1.369	1.375	1.371
H···O=C=O	2.650	2.330	2.316	2.923	2.622
		P2			
Zn−O1	2.606	2.820	2.898	2.384	2.775
Zn−O2	1.944	1.964	1.910	1.976	1.929
H···O=C=O	2.482	2.368	2.152	2.830	2.470
O1−C9	1.309	1.320	1.316	1.308	1.317

[a] **EC**, encounter complex; **TS**, transition structure; **P1**, **P2**, products. For **3′**, see Figure 6. H···O=C=O: distance of one carbon dioxide oxygen to the next hydrogen atom of the ligand sphere.

Table 3. Results of the NBO-Analysis of the Carbonic Anhydrase Model Complexes[a]

	1	**2**	**3**[b]	**4**
		free catalyst		
Q_{Zn}	1.617	1.651	1.612	1.609
Q_{O1}	−1.33	−1.30	−1.3	−1.31
E_{LP}	−0.383	−0.343	−0.369	−0.356
		TS		
Q_{O1}	−1.12	−1.11	−1.12	−1.10
Q_{O2}	−0.75	−0.71	−0.74	−0.73
Q_{O3}	−0.53	−0.58	−0.54	−0.57
Q_C	1.03	1.02	1.02	1.02
WBI(C−O1)	0.366	0.366	0.355	0.388
		P1		
Q_{O1}	−0.80	−0.75	−0.78	−0.78
Q_{O2}	−0.95	−0.97	−0.95	−0.95
Q_{O3}	−0.61	−0.65	−0.62	−0.63
Q_C	0.98	0.99	0.99	0.99
		P2		
Q_{O1}	−0.79	−0.79	−0.76	−0.77
Q_{O2}	−0.89	−0.89	−0.91	−0.90
Q_{O3}	−0.65	−0.67	−0.66	−0.66
Q_C	0.99	1.00	1.00	1.00

[a] Q, charge; WBI, Wiberg Bond Index; E_{LP}, energy of the oxygen p lone pair [eV]. [b] The values for **3** and **3′** are almost identical.

(23) Stewart, J. J. P. *MOPAC93*, QCPE No. 455, version 6.0; Department of Chemistry, Indiana University: Bloomington, IN, 1993.

(24) (a) Klamt, A.; Schüürmann, G. *J. Chem. Soc., Perkin Trans.* **1993**, *2*, 799. (b) Andzelm, J.; Kölmel, C.; Klamt, A. *J. Chem. Phys.* **1995**, *103* (21), 9312. (c) Klamt, A.; Jonas, V. *J. Chem. Phys.* **1996**, *105* (22), 9972.

(25) Clark, T.; Alex, A.; Beck, B.; Chandrasekhar, J.; Gedeck, P.; Horn, A.; Hutter, M.; Martin, B.; Rauhut, G.; Sauer, W.; Schindler, T.; Steinke, T. *VAMP*, Version 7.0a; University of Erlangen−Nürnberg, Department of Chemistry, 1998.

(26) Grev, R. S.; Jansen, C. L.; Shaefer, H. F., III. *J. Chem. Phys.* **1991**, *95*, 5128 and references therein.

(27) Reed, A. E.; Weinstock, R. B.; Weinhold, F. J. *J. Chem. Phys.* **1985**, *83*, 735.

(28) Mauksch, M.; Bräuer, M.; Anders, E. Manuscript in preparation.

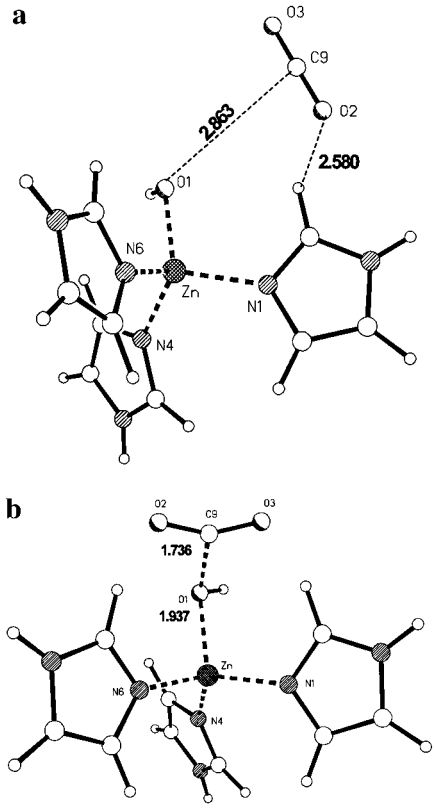

Figure 2. a. Encounter complex **2-EC** for the system **2**/CO_2. b. Transition structure **2-TS** for the system **2**/CO_2.

mutant.[29] The rearrangement can proceed either via the Lindskog (rotation about the CO_2 bond) or Lipscomb mechanism (proton transfer) and has been extensively studied.[1h,1i,8a,8b,9f,10] Calculations suggest that the Lindskog product **P1** is kinetically instable and prefers to stabilize itself by rotation about the CO_2 bond axis to yield the Lipscomb product **P2** which is a thermodynamic "sink" in the reaction path.[10] The Lipscomb alternative (proton-shift) mechanism possesses a significantly higher activation barrier (~28 kcal/mol) and thus seems very unlikely.[10] Work is currently underway to determine whether the nitrogen ligands on zinc (different model compounds) significantly change the relative energies of the two possible reaction pathways (Lindskog/Lipscomb).

Structural Properties. None of the encounter complexes calculated for the model ligands shows a precoordination of CO_2 via an oxygen to the zinc center. All attempts to localize structures with a head-on coordination of CO_2 failed because they collapsed to give **EC**s as shown in Figures 2a and 3a. This finding is in agreement with kinetic investigations on HCA II.[15] In **2-EC** (Figure 2a), the carbon dioxide is attached via hydrogen bonds to the ligands. In the transition structures **TS**, the bicarbonate being formed is already recognizable. **2-TS** (Figure 2b) reveals interesting properties. The C9−O1 distance decreases from 2.864 (**2-EC**) to 1.736 Å (**2-TS**). The OH remains bonded to the zinc center, even though the Zn−O1 distance is elongated (**2-TS**, 1.937; **2-EC**, 1.878 Å). In contrast to this, the distance of the CO_2 oxygen (O2)

(29) Tu, C.; Tripp, B. C.; Ferry, J. G.; Silverman, D. N. *J. Am. Chem. Soc.* **2001**, *123*, 5861.

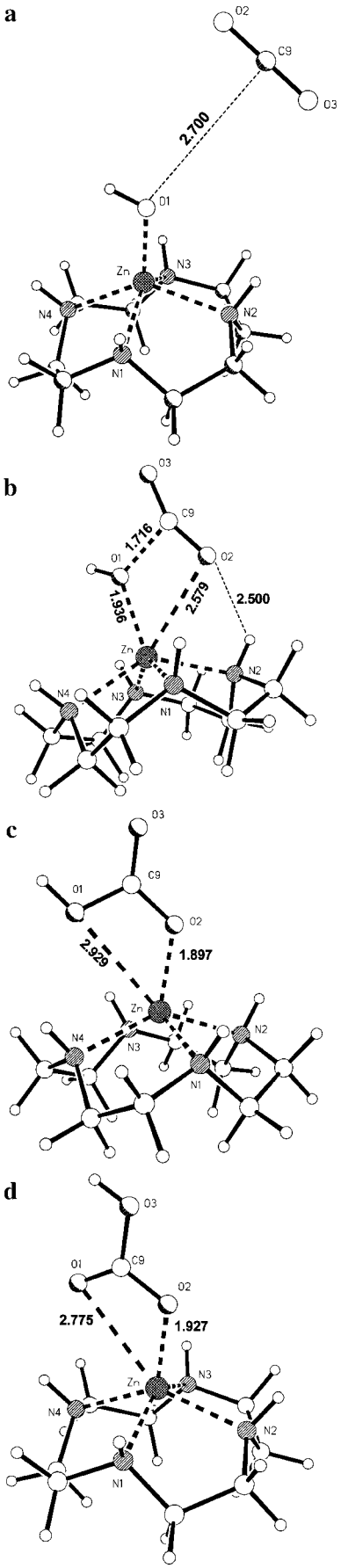

Figure 3. a. Encounter complex **4-EC** for the system **4**/CO_2. b. Transition structure **4-TS** for the system **4**/CO_2. c. Product structure **4-P1** for the system **4**/CO_2. d. Product structure **4-P2** for the system **4**/CO_2.

Table 4. Relative Energies [kcal/mol] of some Stationary Points on the PES of the Carbonic Anhydrase Reaction Cycle for Model Compounds **1**−**4**: B3LYP/6-311+G*//RHF/6-311+G* Results

	$[ZnOH]^+/CO_2$		**1**		**2**	**3**	**3′**	**4**
SR	0		0		0	0	0	0
EC	−34.42	(−33.26)[a]	−4.96	(−4.84)[b]	−3.02	−5.17		−5.32
TS	0.29	(−0.78)[a]	4.25	(4.52)[b]	6.16	4.07		4.01
P1	2.75	(1.08)[a]	−1.58	(−1.87)[b]	−2.31	−1.88	−1.04	−2.96
P2	−10.27	(−12.49)[a]	−8.21	(−8.26)[b]	−8.48	−7.67	−7.55	−8.72
ΔE^a	34.71	(32.64)[a]	9.21	(9.36)[b]	9.17	9.24		9.34
DPE	54.79	(61.74)[a]	148.26	(147.74)[b]	175.90	160.40		166.02

[a] CCSD(T)/6-311+G*//RHF/6-311+G*. [b] B3LYP/6-311+G*// B3LYP/6-311+G*; **SR**, separated reactants; DPE, energy for the deprotonation reaction $[LZnOH_2]^{2+} \rightarrow [LZnOH]^+ + H^+$; ΔE^a, activation energy relative to **EC**.

closest to the zinc center is shortened considerably (**2-EC**, 4.453; **2-TS**, 2.719 Å). Comparable structural properties are calculated for the transition structures of the systems $[Zn([12]aneN_3)OH]^+$ (**3**) and $[Zn([12]ane\ N_4)OH]^+$ (**4**, cf. Figures 3b and Table 2). *These findings indicate that the properties of the transition structure reveal not only the progress of the nucleophilic attack of the free OH electron pair on the CO_2 but also the exchange of the oxygen atoms that coordinate to zinc.* The geometrical details of this transition structure show furthermore that this "coupled motion" is the reason for the low activation energy in the first step of the reaction. The lengthening of the Zn−OH bond increases the (Lewis) acidity of the zinc cation which can then polarize the CO_2 molecule via a beginning O2−Zn contact (Table 3). In the course of the reaction, the CO_2 becomes a more effective C-electrophile with a higher tendency to accept the OH ion. In other words, the zinc cation expands its coordination sphere in order to stabilize a transition structure in which the OH is already on its way to react with the activated CO_2 acceptor.

In all products (**P1**), the bicarbonate is monodentately bound via O2 to the metal ion (Zn−O2 distances: 1.885−1.925 Å). The second oxygen O1 also interacts with the zinc center. However, the Zn−O1 contacts (2.751−3.274 Å) are significantly longer. The same applies for **P2**. Zinc coordinates in all **P2** cases to the oxygen which is trans to the proton (O2). The equilibrium between **P1** and **P2** is the parameter which decides whether the bound bicarbonate decarboxylates (via **P1**) or is replaced via **P2** by an incoming water molecule. The results of the NBO analysis support this assumption (Table 3). When the proton is bound to O3 (**P2**), the negative charge on O2 is reduced, and a smaller interaction with zinc results. In this case, it is easier to remove the O2 oxygen from the metal and to open a coordination site for the incoming water which finally replaces the bicarbonate. Whereas the bicarbonate in **P1** is predominantly bound via O2 to the zinc, O1 still interacts with the metal cation, *thus weakening the O1−C9 bond*. This results in a higher probability for the decarboxylation.

Relative Energies. The relative energies of the stationary points of the catalysts **1**−**4**/CO_2 systems (equivalent to those of Scheme 2) are summarized in Table 4. All complexes react with CO_2 via the same mechanism, and more astonishingly, even quantitative features of the energy profiles are very similar for all four model compounds. The activation energies are listed relative to the separated reactants and, for completeness, are also given relative to the encounter complexes. The reaction proceeds with a small activation barrier (4−6 kcal/mol). The value for complex **2** differs slightly from all other complexes because a strong hydrogen bond hinders the nucleophilic attack (Figure 2a,b). The formation of **P1** is slightly exothermic in all cases (2−3 kcal/mol), whereas the stabilization of **P2** is more pronounced (8−9 kcal/mol).

Table 5. Relative Energies [kcal/mol] for the Stationary Points of Carbonic Anhydrase Reaction Cycle of Model Compounds **1**−**4**: PM3 Results

	1	**2**	**3**	**4**
SR	0.00	0.00	0.00	0.00
EC	−0.71	−0.71		−0.28
TS	19.86	15.57	19.59	19.46
P1	1.16	−0.06	0.00	−0.60
P2	−6.60	−7.95	−8.30	−7.36

Semiempirical Calculations. The application of DFT and ab initio calculations to a large number of such complexes or for larger and more realistic ligand sphere models (as compared to the native enzyme) is not feasible for most research groups at present. Semiempirical calculations seem to be the tool of choice, but their reliability for this type of reaction must first be verified. The borderlines for the performance of PM3 for the carbonic anhydrase catalytic cycle have already been demonstrated.[20] Although the AM1 Hamiltonian has been employed in the majority of past publications, Merz et al. used PM3 in one of their recent investigations. Table 5 compares the PM3 energies with the results from the preceding DFT section. Apart from the activation energies, which are overestimated to a significant extent, the PM3 results are in acceptable qualitative agreement with the DFT results. The activation barriers seem to be overestimated by a constant value of 15 kcal/mol. Complex **2** deviates from this pattern because of the influence of the hydrogen bonds already mentioned. It can be concluded that PM3 provides a relatively reliable basis for energy calculations on the intermediates of the carbonic anhydrase model systems. Extreme caution, however, is required for the estimation of the transition state energy.

Solvent Effects. Because the model systems **3**/CO_2 and **4**/CO_2 were subjected to kinetic measurements in water, we extended our calculations to determine the properties of these systems in that solvent by employing the COSMO model both at the semiempirical (PM3-COSMO) and the ab initio level (B3LYP-COSMO). Tables 6 and 7 summarize the results of the corresponding calculations. Because of the computational demands of solution calculations at the DFT

Table 6. Relative Energies [kcal/mol] for Some Points of the Carbonic Anhydrase Reaction Cycle of Model Compounds **1**−**4** in Aqueous Solution: B3LYP-COSMO and PM3-COSMO Results (in Parentheses)

	1	**2**	**3**	**4**
SR	0.00 (0.00)	0.00 (0.00)	0.00 (0.00)	0.00 (0.00)
EC	−3.92 (8.47)	0.09 (5.07)	−2.81 (−)	−1.92 (1.75)
TS	2.79 (23.85)	1.59 (28.93)	2.58 (25.98)	4.08 (22.15)
P1	−16.66 (1.28)	−13.16 (0.43)	−16.02 (−0.21)	−12.86 (−0.45)
P2	−16.80 (1.34)	−13.19 (0.84)	−15.96 (−0.38)	−12.88 (−0.62)

Table 7. Selected Bond Lengths [Å] for Some Points of the Carbonic Anhydrase Cycle[a]

	3		**4**	
	gas phase	aqueous solution	gas phase	aqueous solution
		free catalyst		
Zn−O1	1.887	1.951	1.890	1.955
		P1		
Zn−O1	2.841	2.882	2.905	2.937
Zn−O2	1.956	2.040	1.951	2.046
		P2		
Zn−O1	2.968	3.079	2.897	3.138
Zn−O2	1.993	2.056	1.992	2.040

[a] Comparison of gas phase and COSMO-solvent calculations; PM3 results.

level of theory, single point estimations of the solvation energy using the gas-phase structures were performed. In contrast to this, full geometry optimizations in water were performed using the faster PM3-COSMO method.

For both model systems, an almost equivalent lengthening of the Zn−O1 and Zn−O2 bonds upon going from the gaseous to the aqueous phase was calculated (Table 7). These structural changes resulting from the influence of the aqueous medium are remarkable but unspecific. They do, however, emphasize the need to optimize the substrate in the solvent in order to obtain accurate energetic data. The following aspects deserve more attention: The encounter complexes of **1**−**4** no longer correspond to minima on the PM3-COSMO potential energy surface (Table 6); the presented values are rough estimates based on single point calculations using the geometries of the preceding gas-phase PM3 calculations. In addition, a futile attempt was made to find an encounter complex for **1** at the B3LYP-COSMO level. This is not surprising when one takes into account the fact that electrostatic interactions between charged and partially charged species should be reduced in an aqueous solution. The relative stability of the product structures reveals much more interesting consequences. Both product structures **P1** and **P2** become almost isoenergetic in water. This supports the thesis that an equilibrium between both modes of bicarbonate complexation should exist. The fact that the products are ∼15 kcal/mol more stable than the reactants for the B3LYP-COSMO results emphasizes once again the necessity of optimizing the reactive species in the solvent. Interestingly enough, the energy of the transition structure is considerably *lowered* (20 kcal/mol in the gas phase vs ∼2−4 kcal/mol in water) upon solvation. Inclusion of solvent effects is obviously necessary in order to achieve a correct description of the energy profile of the catalytic reaction.

Parameters for the Catalytic Activity. In the following section, general parameters, which allow the assessment of the activity of a given model complex, are derived. Qualitative statements regarding the reactivity governing parameters were presented primarily by van Eldik et al.[15] A first attempt to quantify such considerations has been made by Tapia et al.[9d] Complexes **3** and **4** are well suited for a direct comparison of their properties because reliable experimental measurements of their activity are available (Table 1).

The course of chemical reactions is governed by thermodynamic and kinetic effects. Nevertheless, the results in Tables 4 and 6 demonstrate that we are confronted with some difficulties in the case of these enzyme models: The energetic differences between different complexes are negligible in the gas phase as well as in aqueous solution. The stability of the product structures seems to differ only slightly, and a relationship between activation energy and product stabilization which corresponds to the Hammond postulate is not detectable.

A further possibility to classify the reactivity of chemical compounds is the analysis of the charge or orbital control. Unfortunately, the values in Table 3 again show only minor differences in the atomic charge on Zn and O1 in the different complexes. Comparison of the results obtained at both levels of theory (DFT and PM3) does not give completely consistent results. More insight can be obtained by looking at the orbital energies. The Zn−N and Zn−O bonds in the model complexes are significantly ionic in character (For **1**, charges on Zn: 1.62; N, −1.12; O, −1. 33. Bond orders: Zn−N, 0.155; Zn−O, 0.238). For this reason, we find three lone electron pairs on the zinc-bound oxygen, two of them possessing sp character, whereas the remaining one is a pure p-type orbital. Inspection of the orientations and energies of these lone pairs reveals that the p orbital is responsible for the nucleophilic attack on the carbon dioxide. The higher the energy of this p-type lone pair, the easier is the reaction with the LUMO of the carbon dioxide. Within the restriction of similar atomic charges on corresponding atoms, we can thus consider the energy of this lone pair to be an indirect measure of the nucleophilicity of a given model complex. The values in Table 3 indicate a higher nucleophilicity of the OH moiety in complex **4** as compared to that of complex **3**, a fact which is in agreement with the observed reactivity. Surprisingly enough, the differences in the activation barriers do not explain the differences in the catalytic efficiency.

Are there further differences which cause **4** to be a better catalyst than **3**? Inspection of the calculated data reveals that the increased nucleophilicity goes parallel with decreasing O1−C9 distances in the encounter complexes *and* in the transition structures, with a slightly higher (P1, P2) product stabilization, and with an increasing bending (150.06° for **3**, 148.56° for **4**) of the CO_2 substrate. The structural data for the **3-** and **4-EC** complexes clearly show a larger progress in the reaction for **4-EC** as compared to **3-EC** (Table 2). Both complexes exhibit the same Zn−O1 distance (1.93 Å) in the **TS** so that the nucleophilicity at the saddle point of the reaction should be almost equal. The Zn−O2 distance

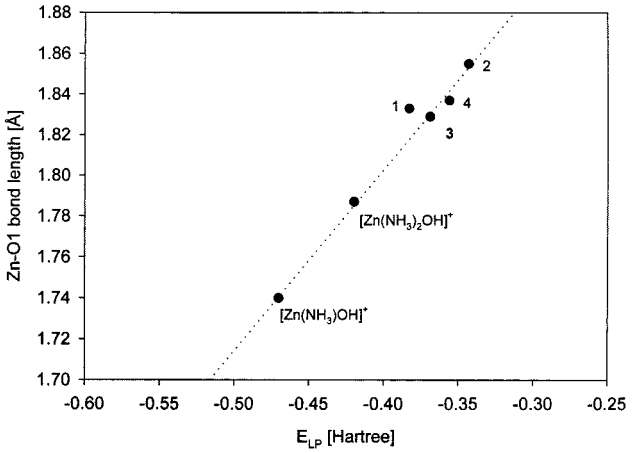

Figure 4. Correlation between E_{PL} (energy of the p lone pair at O1) and the Zn−O1 bond length for model complexes **1**−**4** and some NH_3/[Zn−OH]$^+$ complexes.

is, however, markedly larger in complex **4** than in **3** (**4-TS**, 2.58 Å; **3-TS**, 2.38 Å). This means that the substrate is slightly less polarized by the zinc cation in **4-TS** as compared to **3-TS**. The reason for the larger Zn−O2 distance in complex **4-TS** has its origin in the formation of an additional hydrogen bond and not in a reduced Zn electrophilicity (Figure 3b). The distance of O2 to the closest proton of the macrocyclic ligand is 2.81 Å in **3-TS** and 2.50 Å in **4-TS**. The direct way to the zinc center in **4-TS** is therefore partially blocked by the NH hydrogen. In **4-P2**, the Zn−O2 bond is slightly elongated (**4**, 1.929 Å; **3**, 1.910 Å). This could again cause an enhanced bicarbonate/water exchange rate.

The orbital energy of the lone pair on oxygen has been used so far in order to assess the degree of nucleophilicity of a given model complex. To obtain a reliable energy value, a high level of theory for the calculations is indispensable. The question arises if a simpler approach could give comparable results. It has already been discussed that the zinc cation lowers the nucleophilicity of the hydroxide anion. Changes in the ligand sphere can therefore modify the binding strength of the hydroxide and thus the nucleophilic capacity. The greater the Zn−O1 distance, the stronger will be the characteristic properties of the "pure" hydroxide. In Figure 4, the Zn−O1 bond length in the free catalysts is plotted against the energy of the lone pair on oxygen. Two structures ([Zn(NH$_3$)$_2$OH]$^+$ and [Zn(NH$_3$)OH]$^+$) are included to support this interpretation. The plot shows a good correlation between the values with the exception of complex **1**. An analysis of the structural parameters of this complex shows the presence of a hydrogen bond between the zinc-bound oxygen and a hydrogen of one NH_3 group which obviously causes a slight increase in energy of the lone pair (Figure 5). This correlation of the nucleophilicity with the energy of the p lone pair or vice versa with the Zn−O1 distances allows an interpretation of the extraordinarily long value (2.1 Å) observed in the natural enzyme. This value cannot be caused by the influence of the ligand sphere alone (which is quite similar to the model complex **2**) but is the additive result of a hydroxide stabilizing network of hydrogen bonds. The increased Zn−O1 bond lengths of the free

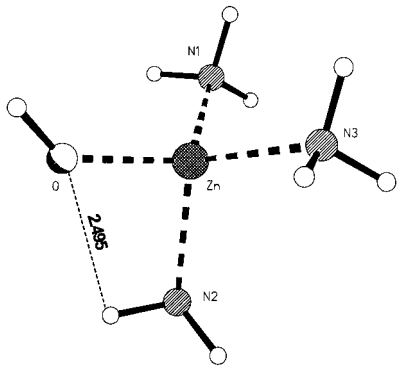

Figure 5. Structure of complex **1**.

catalysts in aqueous solution (Table 7) support this interpretation.

The strength of the Zn−O interaction furthermore determines the acidity of the zinc-bound water. The deprotonation energies (DPE, Table 4) show a direct correlation between the determined order of nucleophilicity and the gas phase basicity. The calculated DPEs in the gas phase do not necessarily have to correlate with the experimentally obtainable pK_a values because solvent effects could cause quite some changes in the thermodynamics of acid−base reactions. Nevertheless, the values in Table 1 show that the general trend is the same in aqueous solution. Because the pK_a value determines the availability of the zinc hydroxide species at a given pH, a compromise between nucleophilicity and basicity must be found. The high activity of complex **4** is accompanied by a pK_a value of 8.1 which is already markedly higher than in the native enzyme.[15]

A further criterion of the catalytic activity is the binding mode of the bicarbonate, because its replacement by water is controlled by this structural parameter to a significant extent in the second part of the catalytic cycle. The greater the bidentate character of the bicarbonate coordination, the smaller is the available space for the interaction of the incoming water with the zinc cation. This assumption is corroborated by the fact that the catalytic activity of carbonic anhydrase analogues *decreases* in the order $Zn^{2+} > Co^{2+} > Ni^{2+} > Cu^{2+}$, which is, according to X-ray analytical results, proportional to the increasing tendency to bind bicarbonate as a bidentate[15] ligand.

The geometrical data in Table 2 for **P2** suggest a tighter binding of the bicarbonate in **4** as compared to **3**. This contrasts with the experimentally established order of activity and is caused by the presence of intramolecular hydrogen bonds. A hydrogen bond between the incoming CO_2 and the ligand ring has already formed in the transition structure **4-TS** (Figure 3b). Further progress of the reaction leads to an arrangement where O2 is bound to the zinc cation and O1 is placed *between* two ring hydrogen atoms (**4-P1**, **4-P2**; Figure 3c,d). In contrast to this, the ligand ring of complex **3** forms strong hydrogen bonds with the bicarbonate in both product structures via the NH moieties (**3-P2**: H1−O, 2.152 Å; H2−O, 3.573 Å. **3′-P2**: H1−O, 2.830 Å; H2−O, 2.879 Å, cf. Figure 6). The trigonal arrangement of the nitrogen atoms makes it harder to find a conformation in which both

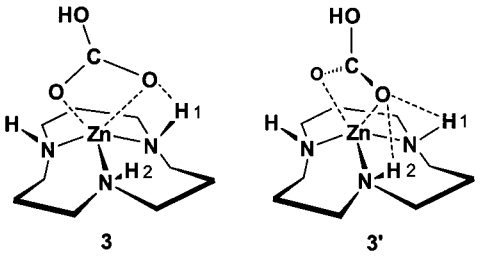

Figure 6. Sterical arrangement of the bicarbonate in **P2** of complex **3** and **3′**.

oxygen atoms are positioned between the hydrogens of the macrocyclic ligands (Figure 6). The hydrogen bonds decrease the ability of the oxygen atom to interact with the zinc cation. A larger Zn−O distance is the consequence. It is quite difficult to find conformers in which O1 is *not* involved in a strong interaction with the ligand, as they are almost isoenergetic with the stationary points found earlier (cf. Table 4, complex **3′**). Figure 6 displays information for the spatial arrangement of the ligands in **3** and **3′**. A comparison of the coordination geometry of **P2** in **3′** with that calculated for complex **4** (Table 2) shows that the correlation of the Zn−O1 distance with the experimentally observed activity is conserved.

The high catalytic activity of complexes such as **4** and **3** is partly due to the steric impediment caused by the macrocyclic ligands. The NH hydrogens interact with the bicarbonate in **P1** and **P2** in order to keep it away from the zinc center. In light of these results, the low activity of model complexes with planar macrocyclic ligands[12c] is easily understood.

To determine which of the product conformers of complex **3** plays the dominant role in aqueous solution, solvent calculations have been carried out. Only structures with strong intramolecular hydrogen bonds could be localized in our gas-phase PM3 calculations. All attempts to localize structures equivalent to **3′** resulted in **3**. However, we expect *intramolecular* hydrogen bonds to play a minor role in aqueous solution because the same interactions can now be caused by the medium. Comparison of the semiempirically calculated geometries in the gas phase and in solution reveal that a monodentate binding mode of the bicarbonate is realized for both complexes in aqueous solution. Zn−O distances of >3 Å are no longer considered to cause significant interactions. Furthermore, this distance is larger in **4-P2** than in **3-P2,** thus allowing a more facile replacement of the bicarbonate by water in case of **4-P2**. This is in agreement with the kinetic data. X-ray analysis of mutated enzymes has shown that zinc coordinates the bicarbonate as monodentate in the natural catalysts.[30] The large Zn−O distance in the native enzyme is presumably caused by a hydrogen bond to Thr199.

Conclusions

We conclude from this investigation that structure−activity relationships for CA model systems can be derived from quantum chemical computations. B3LYP single point calculations with a flexible basis set on structures optimized at the HF level of theory give excellent results for the course of reaction. Except for a systematic overestimation of the activation barrier, acceptable results are also obtained with PM3. The nucleophilic attack of OH^- on the CO_2 proceeds with a low activation energy which is caused by a zinc−CO_2 interaction in these catalysts which polarizes the substrate. The equilibrium between the two products is decisive for the direction of the catalytic reaction. Incorporation of solvent effects into the calculations shows that the reaction is reversible. The energy of the lone pair on oxygen, the DPE, and the Zn−O1 bond length in the free catalysts can serve as a measure for the nucleophilicity of the model system. A high nucleophilicity of $[LZn-OH]^+$ parallels a decreased acidity of the zinc-bound water. Complex **4** reveals a pK_a value of 8.1 which is markedly higher than that in the native enzyme (≈6.8).

The replacement of bicarbonate by water is inhibited by a strong binding of this anion to the zinc center. The Zn−O distances in the product structures can serve as a measure for the capacity of water to replace the product molecule. Whereas the nucleophilicity is almost exclusively dominated by the electron donor capability of the ligand sphere, steric impediments or intramolecular H-bonds contribute to the bicarbonate fixation mode.

On the basis of these calculations and in agreement with experimental results, complexes **3** and **4** are both acceptable models for the carbonic anhydrase. Complex **4** displays the higher activity. If complex **1** could be experimentally accessible, a catalytic activity is to be expected. Complex **2** is (from a structural point of view) a good model for carbonic anhydrase. The stronger donor ability of the sp^2-N-imidazole centers (as compared with the amino ligands of complex **1** (sp^3)) leads to an increased OH nucleophilicity of **2** (Figure 4).

The special suitability of the central zinc cation for this catalytic reaction can be derived from the results of this investigation. If the metal possesses a stronger Lewis acidity or prefers higher coordination numbers than the "moderate" Zn, it would bind the bicarbonate much more strongly in a bidentate manner. This would lead to a lower group transfer activity. The fact that it is a d^{10} element and therefore relatively indifferent to specific ligand arrangements is also important. This property facilitates the fast exchange between different coordination numbers and geometries. This is essential for the most important steps of the catalytic reactions because the zinc center prefers rapid formation of intermediate tetra- and pentacoordinated structures during the nucleophilic attack as well as during the replacement of the bicarbonate.[10]

An efficient model catalyst $[LZn-OH]^+$ should possesses the following properties:

(i) The energy of the p lone pair orbital at the OH moiety should be in the interval between −0.4 and −0.3 eV. This results in Zn−O1 distances between 1.81 and 1.88 Å in the gas phase and is an indirect indicator that a potential catalyst probably possesses sufficient nucleophilicity toward the

(30) Xue, Y.; Vidgren, J.; Svensson, L. A.; Liljas, A.; Jonsson, B.-H.; Lindskog, S. *Proteins* **1993**, *15*, 80.

substrate CO_2. This parameter can be optimized in the desired direction by variation of the ligand sphere.

(ii) The catalyst/CO_2 system must allow fast *intramolecular* ligand rearrangements via five-coordinated structures in the course of the **TS** as well as of the **P1/P2** product formation. This requirement is absolutely necessary and limits the number of acceptable N3 and N4 ligands.

(iii) The intermediate products **P2** must allow the *intermolecular* formation of five-coordinated structures by the attack of external nucleophiles, for example, of H_2O.

(iv) Hydrogen bonds of the bicarbonate in **P2** to the NH hydrogen atoms could favor the catalytic activity.

Acknowledgment. Financial support by the Deutsche Forschungsgemeinschaft (Collaborative Research Center 436, University of Jena), the Fonds der Chemischen Industrie (Germany), and the Thüringer Ministerium für Wissenschaft, Forschung und Kultur (Erfurt, Germany) is gratefully acknowledged. We thank Dr. Tim Clark (Erlangen, Germany) for useful discussions. In addition, we thank the Hewlett-Packard Company for providing us with computer time.

IC0010510